

Full Length Article

Protein kinase D3 conditional knockout impairs osteoclast formation and increases trabecular bone volume in male mice

Samuel D. Burciaga, Flavia Saavedra, Lori Fischer, Karen Johnstone, Eric D. Jensen*

Department of Diagnostic & Biological Sciences, University of Minnesota School of Dentistry, Minneapolis, MN 55455, USA



ARTICLE INFO

Keywords:

Osteoclast differentiation
Protein kinase D
Bone remodeling
Bone resorption

ABSTRACT

Studies using kinase inhibitors have shown that the protein kinase D (PRKD) family of serine/threonine kinases are required for formation and function of osteoclasts in culture. However, the involvement of individual protein kinase D genes and their *in vivo* significance to skeletal dynamics remains unclear. In the current study we present data indicating that protein kinase D3 is the primary form of PRKD expressed in osteoclasts. We hypothesized that loss of PRKD3 would impair osteoclast formation, thereby decreasing bone resorption and increasing bone mass. Conditional knockout (cKO) of *Prkd3* using a murine Cre/Lox system driven by *cFms-Cre* revealed that its loss in osteoclast-lineage cells reduced osteoclast differentiation and resorptive function in culture. Examination of the *Prkd3* cKO mice showed that bone parameters were unaffected in the femur at 4 weeks of age, but consistent with our hypothesis, *Prkd3* conditional knockout resulted in 18 % increased trabecular bone mass in male mice at 12 weeks and a similar increase at 6 months. These effects were not observed in female mice. As a further test of our hypothesis, we asked if *Prkd3* cKO could protect against bone loss in a ligature-induced periodontal disease model but did not see any reduction in bone destruction in this system. Together, our data indicate that PRKD3 promotes osteoclastogenesis both *in vitro* and *in vivo*.

1. Introduction

Proper maintenance of skeletal bone is of great importance to quality of life. Excessive bone destruction underlies many distinct pathologic conditions including cancer-associated bone disease, periodontal disease, osteoporosis, peri-implant osteolysis and arthritis [1]. In these, excessive bone destruction leads to fractures, bone and joint destruction, failure of dental or orthopedic implants and hypercalcemia. Bone loss occurs by the action of specialized cells called osteoclasts, which are large, multinucleated cells formed by fusion of mononucleated progenitors of the monocyte/macrophage lineage [2,3]. Two of the key regulators of osteoclast formation are RANKL [4] (receptor activator of NF- κ B ligand) and M-CSF [5,6]. RANKL, a cytokine produced by osteoblasts, osteocytes [7] and synovial fibroblasts [8] recruits mononucleated osteoclast precursors, drives commitment to the osteoclast lineage, and promotes differentiation and cell-cell fusion into mature multinucleated osteoclasts. Additionally, various immune cells secrete RANKL and other cytokines to impact osteoclastogenesis, particularly during inflammatory conditions [9,10]. Efficient osteoclast formation by M-CSF and RANKL requires additional co-stimulatory signals

mediated by DAP12 and Fc γ [11], which are not sufficient on their own for osteoclastogenesis. M-CSF and RANKL activate intracellular signaling pathways including MAPKs, PI3K/AKT, BTK and NF- κ B, leading to increased expression of the NFATc1 transcription factor [12], which acts as a master regulator of osteoclast formation [13]. Once differentiated into mature osteoclasts, they bind to the bone surface via integrins [14,15] and sequester the underlying space via the sealing zone [16], which is formed by a large podosome-based structure called the actin ring [17]. Osteoclasts then secrete acids and proteases into the resorption lacuna to demineralize the hydroxyapatite mineral and degrade the collagen-rich bone extracellular matrix, leading to bone loss or resorption [18,19]. Better understanding the cellular and molecular pathways regulating osteoclast formation from mononucleated precursors and their subsequent bone resorptive activities is anticipated to lead to new therapies for better clinical management of osteolytic processes and to improved patient health.

We have identified protein kinase D (PRKD) as a novel regulator of osteoclasts [20–22]. Protein kinase D is a family of three closely related serine/threonine kinases: PRKD1 (PKC μ) [23,24], PRKD2 [25] and PRKD3 (PKC ν) [26] that are placed into a novel subgroup of the

* Corresponding author.

E-mail address: jens0709@umn.edu (E.D. Jensen).

<https://doi.org/10.1016/j.bone.2023.116759>

Received 17 January 2023; Received in revised form 15 March 2023; Accepted 4 April 2023

Available online 11 April 2023

8756-3282/© 2023 Elsevier Inc. All rights reserved.

calcium/calmodulin-dependent protein kinase superfamily based on sequence homology of their catalytic domain [27]. The PRKD proteins are composed of an N-terminal regulatory domain containing two cysteine-rich zinc finger domains and an autoinhibitory pleckstrin homology domain, and a C-terminal kinase catalytic domain. See [28–30] for review of PRKD structure, regulation and functions. In the classical PRKD activation pathway [31,32], receptor-activated pathways stimulate phospholipases to cleave phosphatidylinositol 4,5-bisphosphate into diacylglycerol (DAG) and stimulate novel protein kinase C isoforms (nPKC). PRKD is recruited to the plasma membrane via the DAG-binding activity of the PRKD zinc-finger domains, where it becomes phosphorylated at two serines (Ser744 and Ser748 of mouse PRKD1) [33] in the kinase activation loop by nPKC [34]. Subsequent work has suggested that autophosphorylation by PRKD itself may be the main mechanism of Ser748 phosphorylation [35]. PRKD1 and 2 also possess an autophosphorylation site at Ser916 [36] near their C-terminus that has often been used as a marker of PRKD catalytic activity. Activation of PRKD isoforms can also involve tyrosine phosphorylation [37,38], and there are reports of PRKD activation by additional mechanisms [39–42]. Once activated, PRKD proteins phosphorylate an array of substrates on a conserved peptide motif [43,44] to regulate activity of their targets and influence cellular behavior. PRKD and its targets have been implicated in diverse cellular processes [28–30] including actin cytoskeletal dynamics [45,46], cellular survival/apoptosis [37], proliferation [47], differentiation, regulation of gene expression and vesicle trafficking [48]. Alterations in PRKD activity or expression have been connected to an array of cancers [28,49,50] and small-molecule PRKD inhibitors are being investigated for potential applications against cancers and other human diseases [51].

Given their many functions, we sought to determine if and how PRKD impacts osteoclasts. We made use of PRKD kinase chemical inhibitors in osteoclast cell culture to discover that PRKD activity is required for fusion of committed mononucleated osteoclast precursors into multinucleated osteoclasts and for maintenance of the actin ring formed by mature osteoclasts as part of their bone resorptive machinery [20,21]. Subsequently, a phosphoproteomics-based approach was used to identify the histone deacetylase 5 transcriptional co-repressor as an endogenous substrate of protein kinase D in osteoclasts [22]. Although these studies demonstrated the involvement of PRKD protein family in osteoclasts, important unanswered questions include exactly which of the three PRKD kinases are involved in osteoclastogenesis and whether loss of PRKD in osteoclasts impacts skeletal physiology *in vivo*. Since loss of PRKD function impairs osteoclast formation in culture, we hypothesized that conditional deletion of PRKD in osteoclasts should reduce osteoclast formation and bone resorption, likely increasing bone volume. In the current study we describe results demonstrating that conditional deletion of protein kinase D3 in osteoclast-lineage cells impairs osteoclast formation in culture and in the intact skeleton, leading to increased trabecular bone volume in male mice at 3 and 6 months of age.

2. Materials & methods

2.1. Mouse breeding and genotyping

Mice containing conditional alleles of *Prkd2* and *Prkd3* were previously described [52], and were kindly provided by Sho Yamasaki. They were mated to *cFms-Cre* transgenic mice purchased from the Jackson Laboratory. *Prkd^{flox/flox}; cFms-Cre*-positive mice are referred to as *Prkd* conditional knockout (*Prkd* cKOs). *Prkd^{flox/flox} Cre*-negative mice, referred to as *Prkd* flox, were used as normal controls. The presence of *Prkd* flox and wild-type alleles and the *c-Fms-Cre* transgene were detected by PCR against genomic DNA isolated by tissue biopsy at the distal tail. Sequences of the primers used for genotyping are provided in Supplemental Table 1. Amplification products were resolved by agarose gel electrophoresis and stained using SybrSafe DNA Stain (Thermo Fisher).

2.2. Mouse osteoclast cultures

Murine bone marrow-derived osteoclasts were isolated and cultured according to published protocols [22,53]. Briefly, bone marrow was flushed from the tibiae and femurs of mice at 2–4 months age, incubated in ACK red blood cell lysis buffer, then plated to tissue culture dishes overnight in phenol red-free α -MEM supplemented with 5 % fetal bovine serum, penicillin-streptomycin, and 1 % CMG14-12 cell supernatant [54] as a source of M-CSF. The following day, the non-adherent cell population containing monocytes was re-plated to tissue culture plates at 100,000 cells/cm² and cultured for 48 h. Any non-adherent cells were then removed. The remaining adherent bone marrow macrophages, BMMs, were further cultured in media containing M-CSF and 20 ng/mL RANKL (R&D Systems). This media was changed every 2 days. Cells were fixed with 4 % formaldehyde solution, permeabilized using 0.1 % triton X-100 in PBS and stained for TRAP to visualize osteoclast differentiation, rhodamine-phalloidin to assess actin ring morphology, and DAPI to visualize nuclei. Osteoclasts were defined as TRAP-positive cells containing ≥ 3 nuclei, and typically appear 3–4 days after RANKL stimulation. Cells were photographed on an Olympus IX70 inverted microscope and photographed with a DP71 digital camera using light and epifluorescence imaging. Image processing and analysis was performed using Adobe Photoshop and NIH ImageJ software.

Resorption assays were performed as described [55,56]. Bone marrow monocytes were seeded onto bovine bone slices (Immunodiagnostic Systems) and cultured until the third day of RANKL stimulation. They were then switched to α MEM at pH 6.8 supplemented with M-CSF and RANKL. At day 6 of the culture, cells were removed from the bone slices using a cotton swab. The bone slices were stained with hematoxylin for 10 s then swabbed vigorously to remove excess background staining and reveal resorption pits. Bone slices were mounted in glycerol and observed using reflective light microscopy on an Olympus BX51 microscope.

2.3. RNA isolation and real-time qPCR

RNA was harvested from cell cultures in triplicate using Trizol reagent (Thermo Fisher) according to the manufacturer's recommended protocol. RNA was quantified using UV spectroscopy and used for reverse transcription with the iScript cDNA synthesis kit (Bio-Rad). Relative gene expression was then determined using quantitative real-time PCR. Amplification reactions were performed using iTaq Sybr Green Supermix (Bio-Rad) run on a CFX Connect Real Time PCR System. Target genes were normalized to expression of *Hprt1*. Primer sequences used for qPCR are given in Supplemental Table 1.

2.4. Cell transfection and Western blotting

HEK293T cells were transfected using Fugene HD (Promega) transfection reagent by the recommended protocol with plasmids encoding epitope-tagged mouse PRKD1-GFP, PRKD2-FLAG and PRKD3-MYC-FLAG. HEK293T and osteoclast cellular proteins were harvested using ice-cold NP40 lysis buffer (50 mM Tris pH 7.4, 250 mM NaCl, 5 mM EDTA, 1 % NP40) supplemented with protease and phosphatase inhibitors (Thermo Fisher). Lysates were cleared by centrifugation for 10 min at 12,000 $\times g$ at 4 °C. Proteins were resolved by SDS-PAGE and transferred to PVDF membranes (Millipore). TBST +3 % BSA was used to block the membrane and for primary antibody incubations overnight at 4 °C. Blots were washed with TBST, then incubated with HRP-conjugated secondary antibodies (Advansta) diluted in TBST + 5 % nonfat milk for 1 h at room temperature. Bands were visualized using WesternBright Sirius chemiluminescence substrate (Advansta) on a ChemiDoc Touch imaging system (Bio-Rad). The antibodies used were: protein kinase D1 (Cell Signaling #2052, Cell Signaling #90035), protein kinase D2 (EMD-Millipore ST-1042, Bethyl A300-074A, Cell Signaling #8188, Abcam Ab51250), protein kinase D3 (Cell Signaling

#5655), α -tubulin (Cell Signaling #2144).

2.5. Micro computed tomography (μ CT) imaging and analysis

Femurs were dissected from freshly euthanized mice, fixed overnight in formalin and stored in 70 % ethanol. Bones were scanned on a Nikon XT H 225 μ CT instrument operating at 120 kV, 61 μ A, 1 mm aluminum filter, 720 projections, 2 frames per projection, and an integration time of 708 milliseconds. The resulting images had an isotropic pixel resolution of 8.85 μ m. Scans were reconstructed using CT Pro 3D software (Nikon Metrology) and converted to bitmaps using Studio MAX 3.4 (Volume Graphics GmbH). Morphometric analysis was performed using CT-Analyzer software (Bruker microCT). The region of interest (ROI) for trabecular bone analysis at the distal metaphysis started 0.7 mm proximal to the growth plate and extended 1.5 mm proximally towards the diaphysis for the 4 week samples, and 2.0 mm for 12 week and 6 month samples. The region for cortical bone analysis was a 0.5 mm section at the mid-diaphysis. Automated contouring was used to determine the region of interest for both trabecular and cortical bone, with global thresholding used to segment bone from surrounding tissue for analysis.

2.6. Histological staining

Mouse femurs were fixed overnight in formalin, decalcified by incubation in 10 % EDTA at 4 °C, embedded in paraffin, and sectioned by standard methods. Slides were then stained with hematoxylin and eosin (H&E) or stained for TRAP activity with methyl green counterstaining. The stained sections were mounted in permount and examined on an Olympus BX51 microscope at 4 \times magnification for H&E staining and 20 \times magnification for TRAP staining. Quantitative histomorphometric analysis of the slides was performed using NIH ImageJ and Adobe Photoshop with the investigator blinded to sample sex and genotype. For H&E staining the number of animals analyzed: male flox = 8, male cKO = 7, female flox = 7, female cKO = 8. For each animal the trabecular bone area and total area were measured in the secondary spongiosa from a single section. For TRAP staining, the number of animals analyzed: male flox = 9, male cKO = 8, female flox = 7, female cKO = 5. 3–4 microscope fields within the secondary spongiosa were analyzed per specimen. To determine average bone perimeter per osteoclast (B.Pm/Oc), the length of trabecular bone covered by each individual osteoclast was manually measured, with between 221 and 598 cells measured per group.

2.7. Serum Crosslaps (CTX-1) ELISA

Serum was isolated by centrifugation of whole blood collected at the time of euthanasia and stored at –80 °C until analysis. The presence of CTX-1 was measured using the Serum Crosslaps (CTX-1) ELISA kit (Immunodiagnostic Systems) according to the manufacturer's recommended protocol, with each biological sample assayed in duplicate.

2.8. Ligature-induced periodontal disease model

Ligature-induced periodontitis was performed as previously reported [57]. Mice at 10 weeks of age were placed under ketamine/xylazine anesthesia. A size 5–0 silk suture was ligated around the right second maxillary molar of each mouse. Five days later, the mice were euthanized. Their maxillae were then harvested, fixed overnight in 4 % formaldehyde, and used for μ CT imaging.

2.9. Experimental replication and statistical analysis

Cell culture experiments were performed at least three times with 3–4 technical replicates per group. Within each experiment the control and knockout cells were always from mice of the same sex and age. Quantitative data presented for cell culture studies show results from

single representative experiments and are graphed as the mean + standard deviation. Data processing, analysis and statistical testing was performed using Excel (Microsoft) or R Studio (Posit) statistical software. Comparisons between two groups were performed using Student's *t*-test. Significance of the actin ring population distributions in Fig. 2E were tested using the Chi-Squared test.

2.10. Ethics statement

Mice were kept in University of Minnesota Research Animal Resources housing and maintained according to applicable NIH and University of Minnesota guidelines. All experimental procedures received prior approval from the University of Minnesota IACUC (Protocols 2010-38523A and 1710-35270A).

3. Results

3.1. Protein kinase D3 cKO impairs osteoclast formation in vitro

In our previous work, we reported expression of PRKD3 in osteoclasts [21,22]. To test its functional role, we generated mice in which the *Prkd3* gene was conditionally deleted in osteoclasts. To achieve this, we interbred mice carrying the *c-Fms-Cre* transgene, which is expressed in osteoclasts and their macrophage precursors, as well as dendritic cells and bone marrow granulocytes [58], with *Prkd3^{flox}* mice. The *Prkd3^{flox}* mice were previously used successfully for conditional knockout of *Prkd3* in T-cells [52]. From these crosses, we obtained homozygous *Prkd3^{flox/flox}* Cre-negative (*Prkd3* flox) control mice and *Prkd3^{flox/flox}* *c-Fms-Cre* conditional knockout (*Prkd3* cKO) mice. *Prkd3* flox and cKO mice were born at the expected Mendelian ratios, with the caveat that *Prkd3* and the *c-Fms-Cre* transgene displayed genetic linkage, indicating that they are both located on mouse chromosome 17 separated by 15 cM genetic distance based on their recombination frequency. To verify that the Cre/LoxP recombination system was working as expected, we performed PCR on genomic DNA from distal tail biopsies and from osteoclast cultures of *Prkd3* mice (Fig. 1A). Genomic DNA from a heterozygous *Prkd3^{flox/+}* mouse tail in lane 6 acted as a positive control and size standard for the *Prkd3* wild-type (wt) allele and *Prkd3^{flox}* allele, which is larger due to the LoxP sequences. PCR on tail biopsy DNA from Cre-negative *Prkd3^{flox/flox}* and Cre-positive *Prkd3* cKO mice showed the *Prkd^{flox}* allele (lanes 1–2). Osteoclast cultures from the same mice (lanes 3–4) revealed that in cKO osteoclasts the *Prkd^{flox}* allele was nearly absent, having been efficiently replaced by the deletion allele. We did not detect loss of the *Prkd^{flox}* allele or formation of the deletion allele in the tail biopsy DNA. These data indicate the expected CRE-mediated excision of the *Prkd3* gene in osteoclasts. RT-PCR using primers specific for the region expected to be deleted in the cKO showed a strong reduction of *Prkd3* mRNA from the cKO osteoclast cultures ($p = 0.002$) (Fig. 1B). No change in *Prkd1* or *Prkd2* mRNA expression was detected in these cultures (not shown). Western blotting revealed that PRKD3 protein was undetectable in *Prkd3* cKO osteoclasts cultured from either male or female mice (Fig. 1C). Together these data establish that our *Prkd3^{flox}*; *c-Fms-Cre* system successfully deletes PRKD3 expression in osteoclasts.

We then examined differentiation of *Prkd3* cKO and flox control osteoclasts from bone marrow monocytes stimulated with M-CSF and RANKL. There was no difference in the number of nuclei present from day –1 (the day prior to RANKL addition) through day 3 of RANKL stimulation, where pre-osteoclasts were fusing into multinucleated osteoclasts (Fig. 2A). These data suggest that *Prkd3* cKO has little impact on proliferation or survival of the cells at these stages. We next examined whether it impacted induction of bone marrow macrophages into TRAP-positive osteoclasts. Staining the cultures for TRAP (Fig. 2B) and DAPI (not shown) after three to four days stimulation with RANKL revealed the *Prkd3* flox cells formed large, multinucleated osteoclasts, whereas the TRAP-positive multinucleated osteoclasts formed in *Prkd3* cKO

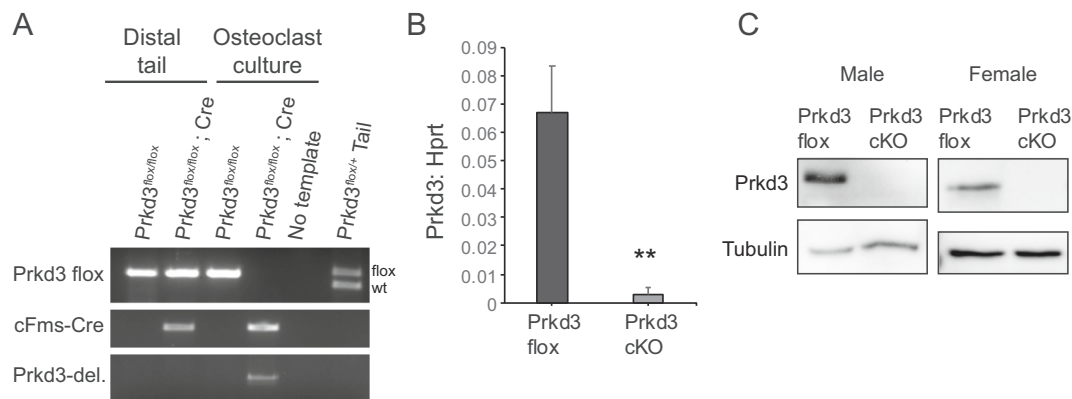


Fig. 1. Conditional knockout of *Prkd3* in osteoclasts (A) PCR on genomic DNA isolated from distal tail biopsies and primary osteoclast cultures from the same mice showing loss of the *Prkd3*^{flox} allele and formation of the *Prkd3*^{deletion} allele specifically in *cFms-Cre*-positive cKO osteoclasts. No-template negative control and *Prkd3*^{flox/+} tail DNA as a size standard are shown at right. Real-time qPCR of *Prkd3* mRNA expression (B) and Western blots for PRKD3 protein (C) in osteoclast cultures from *Prkd3* flox and *Prkd3* cKO mice. ***p* < 0.005.

cultures were markedly smaller and contained significantly fewer nuclei (Fig. 2B–C). Staining the actin cytoskeleton revealed altered actin cytoskeletal architecture, with fewer *Prkd3* cKO osteoclasts containing well-formed peripheral actin belts that are important for the sealing zone and resorption of the underlying bone (Fig. 2D–E). Finally, we cultured cells on bone slices and compared their bone resorptive capacity. Generation of resorption pits was impaired in *Prkd3* cKO cultures, leading to significant reductions in the average pit size and the total area resorbed compared to *Prkd3* flox controls (Fig. 2F). Comparable results were observed in each of these assays using cells from male or female mice. Representative data from single experiments are shown; any differences between male and female *Prkd3* flox cells were not reproducible between experiments. These results together indicate that *in vitro* osteoclast differentiation, actin cytoskeleton organization, and bone resorptive capacity are diminished by loss of PRKD3 in osteoclasts.

3.2. Protein kinase D2 cKO has little effect and shows limited expression in osteoclasts

In addition to PRKD3, in our previous paper we also reported that osteoclasts express PRKD2 but not PRKD1 [21]. Consequently, we asked whether conditional deletion of the *Prkd2* gene using *cFms-Cre* affected osteoclasts. We showed the expected excision of the *Prkd2* genomic DNA locus and loss of *Prkd2* mRNA in cKO osteoclasts (Supplemental Fig. 1A–B). However, we were unable to detect any *in vitro* phenotype in the *Prkd2* cKO osteoclasts (Supplemental Fig. 1D–F). We characterized *Prkd2/Prkd3* double cKO osteoclasts, finding that they show impaired osteoclast formation in culture comparable to that of the *Prkd3* single cKO cells (data not shown).

Results of western blotting against PRKD2 in control and *Prkd2* cKO cultures, as well as the lack of a phenotype raised questions of whether it is actually expressed in osteoclasts. Western blots using PRKD2 antibodies ST-1042 and A300-074A did show bands at the expected molecular weight of approx. 120 kDa in *Prkd2* flox cells (Supplemental Fig. 1C), but the bands were not changed in *Prkd2* cKO (or *Prkd3* cKO, not shown) osteoclasts. Blotting the same osteoclast lysates with two other commercial PRKD2 antibodies, #8188 and Ab51250, did not show any bands near 120 kDa (data not shown). A number of commercial PRKD antibodies are known to be cross-reactive between the PRKD proteins, and various other technical issues have been described with others [59–62]. These concerns led us to carefully test the specificity of our PRKD antibodies and their ability to detect PRKD proteins in osteoclasts by western blot (Supplemental Fig. 2A). As positive controls to validate the sensitivity and specificity of our antibodies, we transfected HEK293T cells with plasmids encoding epitope-tagged mouse PRKD1, PRKD2 and PRKD3 and performed western blots. Alongside these, we

ran lysates from mouse osteoclast cultures at Day 0 (prior to RANKL addition) or at 3 days RANKL stimulation. The PRKD1 CS-2052 polyclonal antibody is reported by its manufacturer as cross-reactive to PRKD1 and PRKD2. This antibody readily detected overexpressed PRKD1 and 2 proteins and a 120 kDa band in untransfected HEK293T cells. Cells transfected with PRKD3 showed a mild increase in the 120 kDa band compared to untransfected cells suggesting that the antibody may also be reactive against mouse PRKD3 to some extent. PRKD1 CS-2052 sometimes detected a weak 120 kDa band in osteoclast lysates. PRKD1 antibody CS-90035 appears to be more specific for PRKD1 than CS-2052. It readily detected 150 kDa and 120 kDa bands that presumably represent PRKD1-GFP and endogenous PRKD1 in HEK293T cells. We did not see any potential PRKD bands in osteoclasts with this antibody even after long exposures. PRKD2 antibodies ST-1042 and A300-074A were both raised against the same peptide epitope. Both demonstrate cross-reactivity against overexpressed mouse PRKD1, PRKD2 and PRKD3. In osteoclasts they detected bands at 120 and 200 kDa, but as mentioned, neither band was reproducibly affected in *Prkd2* cKO or *Prkd3* cKO cultures. Two additional PRKD2 antibodies, CS-8188 and Ab51250, appear to be more specific based on the HEK293T cell overexpression. They did not show any bands near 120 kDa in control or cKO osteoclasts. PRKD3 antibody CS-5655 appears to be specific for PRKD3 in our tests. It readily detects overexpressed and endogenous PRKD3 in HEK293T cells and in osteoclasts at both timepoints. The A300-319A PRKD3 antibody used in our earlier publication has been discontinued by the manufacturer so was not tested here. In summary, the PRKD3 CS-5655 antibody shows a good specificity profile and indicates expression of PRKD3 in control osteoclasts and loss of *Prkd3* in cKO cells (Fig. 1C). Neither PRKD1 nor PRKD2 is detected in osteoclasts using the high specificity antibodies; possible PRKD bands are only detected in osteoclasts with the more promiscuous antibodies. qPCR using primer pairs predicted to be specific for the intended target gene confirm *Prkd3* as the most abundant, with low expression of *Prkd1* and *Prkd2* mRNAs (Supplemental Fig. 2B). We saw a similar pattern of *Prkd* expression (*Prkd3* > *Prkd2* > *Prkd1*) in several sets of RNA-Seq performed on osteoclast mRNA (data not shown). Collectively, our interpretation of these western blot and mRNA data is that PRKD3 is the primary PRKD protein present in osteoclasts, while PRKD1 and PRKD2 have limited or absent expression.

3.3. Protein kinase D3 conditional knockout in osteoclasts increases trabecular bone mass in male mice

From the *in vitro* data demonstrating impaired osteoclasts from *Prkd3* cKO, we then tested whether this impacted bone *in vivo*, with the hypothesis that reduced osteoclast activity in the *Prkd3* cKO mice should

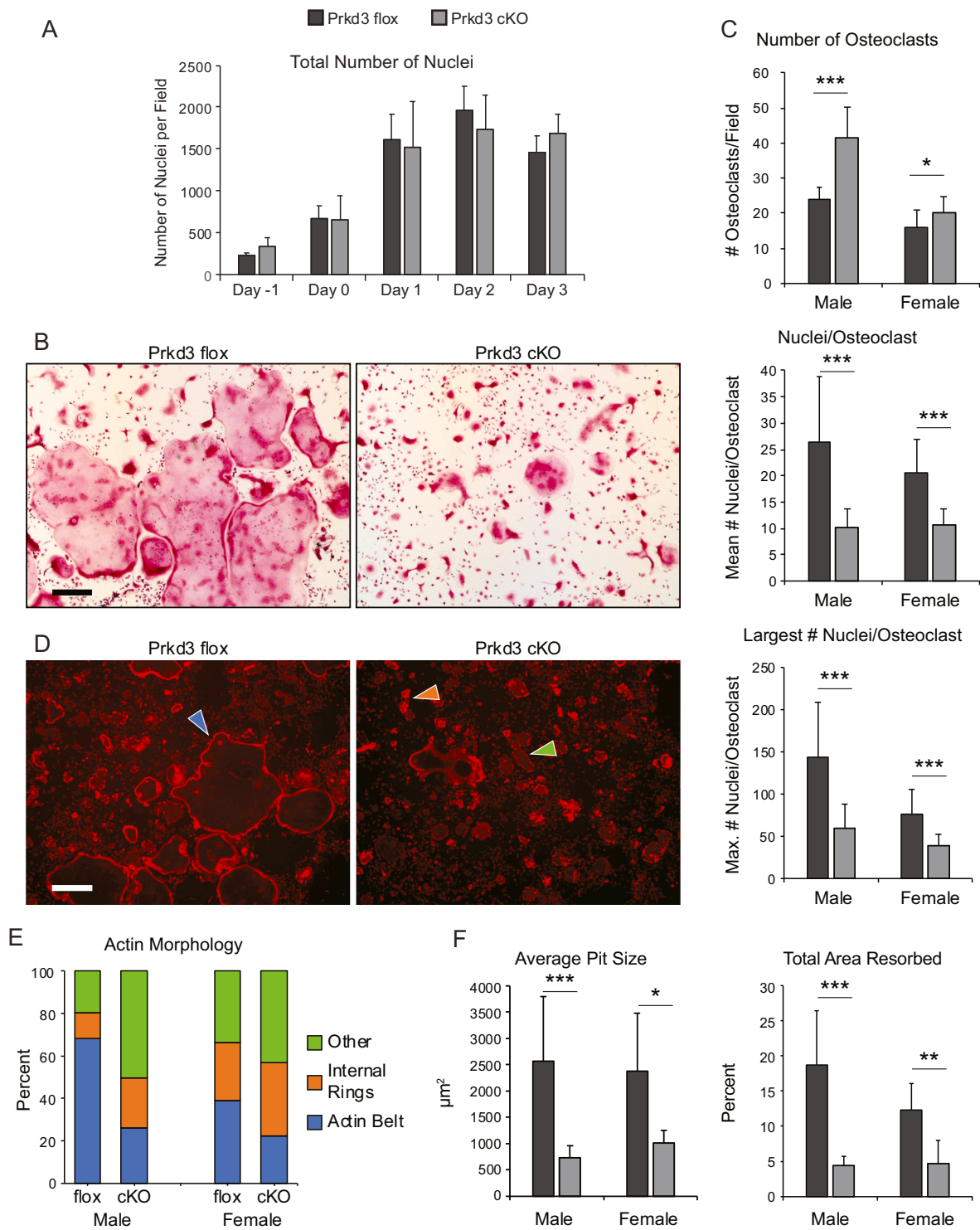


Fig. 2. *In vitro* phenotypes of *Prkd3* cKO osteoclast cultures (A) The number of nuclei on the indicated times of culture relative to RANKL addition, comparing *Prkd3* flox (dark bars) and cKO (light bars) cultures. Total number of nuclei per field were visualized by DAPI staining. (B) TRAP staining of *Prkd3* flox and cKO osteoclast cultures. Scale bar = 250 μ m (C) Quantitative analysis of number of osteoclasts (TRAP-positive multinucleated cells with 3-or-more nuclei) per field and nuclei per osteoclast (D) Rhodamine-phalloidin staining for actin cytoskeleton. Examples of cells showing mature actin belts (blue arrowhead), smaller internal rings (orange arrowhead), and other actin morphology (green arrowhead) are indicated. Scale bar = 400 μ m (E) quantitative analysis of the percentage of osteoclasts with each actin morphology. The population distributions in both sexes show statistically significant differences by the Chi-squared test ($p < 5 \times 10^{-20}$ for males and $p < 0.001$ for females) (F) Average resorption pit size and total resorbed area produced by *Prkd3* flox and cKO osteoclasts cultured on bone slices. * $p < 0.05$, ** $p < 0.005$, *** $p < 0.0005$. (For interpretation of the references to colour in this figure legend, the reader is referred to the web version of this article.)

decrease bone resorption and increase bone volume. We collected mice at 1- and 3- and 6- months ages. There was no detected phenotype associated with *Prkd3* knockout in the body mass or body length at any timepoint (Fig. 3A). To assess skeletal phenotypes, we performed microCT analysis of cortical bone at the femoral midshaft and trabecular bone at the distal femur. At 1-month (4-week) timepoints, there was no significant difference between *Prkd3* flox and cKO mice of either sex at either site (Fig. 3B), although trends towards very slight increases in BV, BV/TV, Tb.N and decreased Tb.Sp were seen. At 3-months (12-weeks), we noted significant changes in each of those parameters in male mice, with increases in bone volume (BV), tissue volume (TV), BV/TV, and in

the number of trabeculae (Tb.N). Trabecular separation (Tb.Sp) trended to a 10 % reduction ($p = 0.083$) (Fig. 4A–B). The cortical cross-sectional bone area (Ct.B.Ar) showed a small but statistically significant increase, while cortical thickness (Ct.Th) was slightly decreased (not significant). There were no apparent or statistically significant differences between female *Prkd3* flox and cKO mice. Representative 2-dimensional radiographic images from the μ CT of *Prkd3* male mice are shown in Fig. 4B. These specific samples were chosen for having BV/TV parameters near to their group means. Visually, we note increased abundance of trabeculae in the knockouts extending more proximally towards the diaphysis. Similar patterns were observed at 6-months age, where *Prkd3*

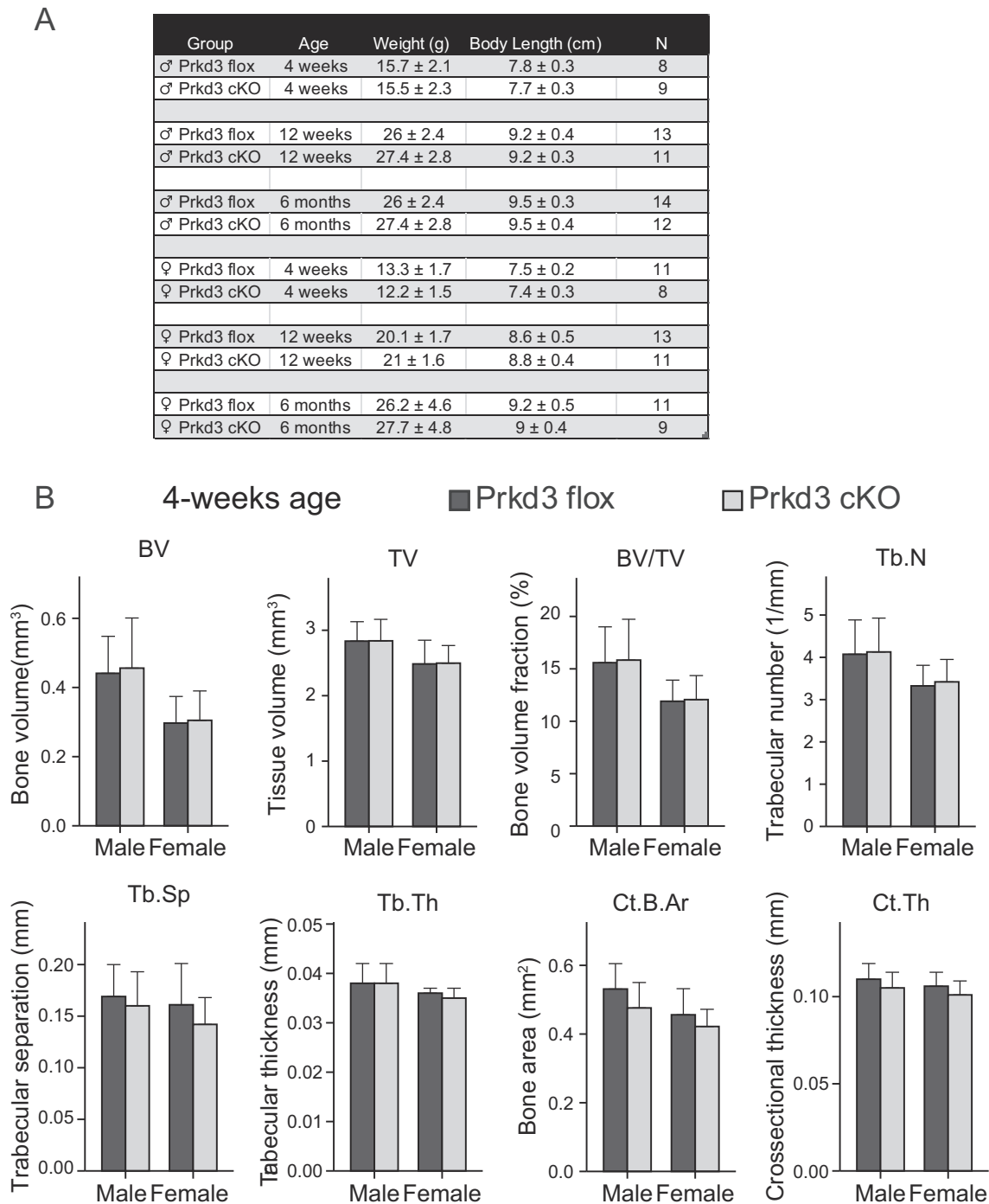


Fig. 3. Phenotypes of *Prkd3* cKO mice (A) Body weight and length for mice of the indicated genotypes and ages. No statistically significant differences between *Prkd3* flox and cKO of the same sex and age were observed. (B) μ CT analysis of *Prkd3* flox (dark bars) and *Prkd3* cKO (light bars) mice at 4-weeks age. Cortical analysis was performed at the mid-diaphysis, while trabecular analysis was done at the distal femur. Number of individuals analyzed by μ CT is indicated in Fig. 3A.

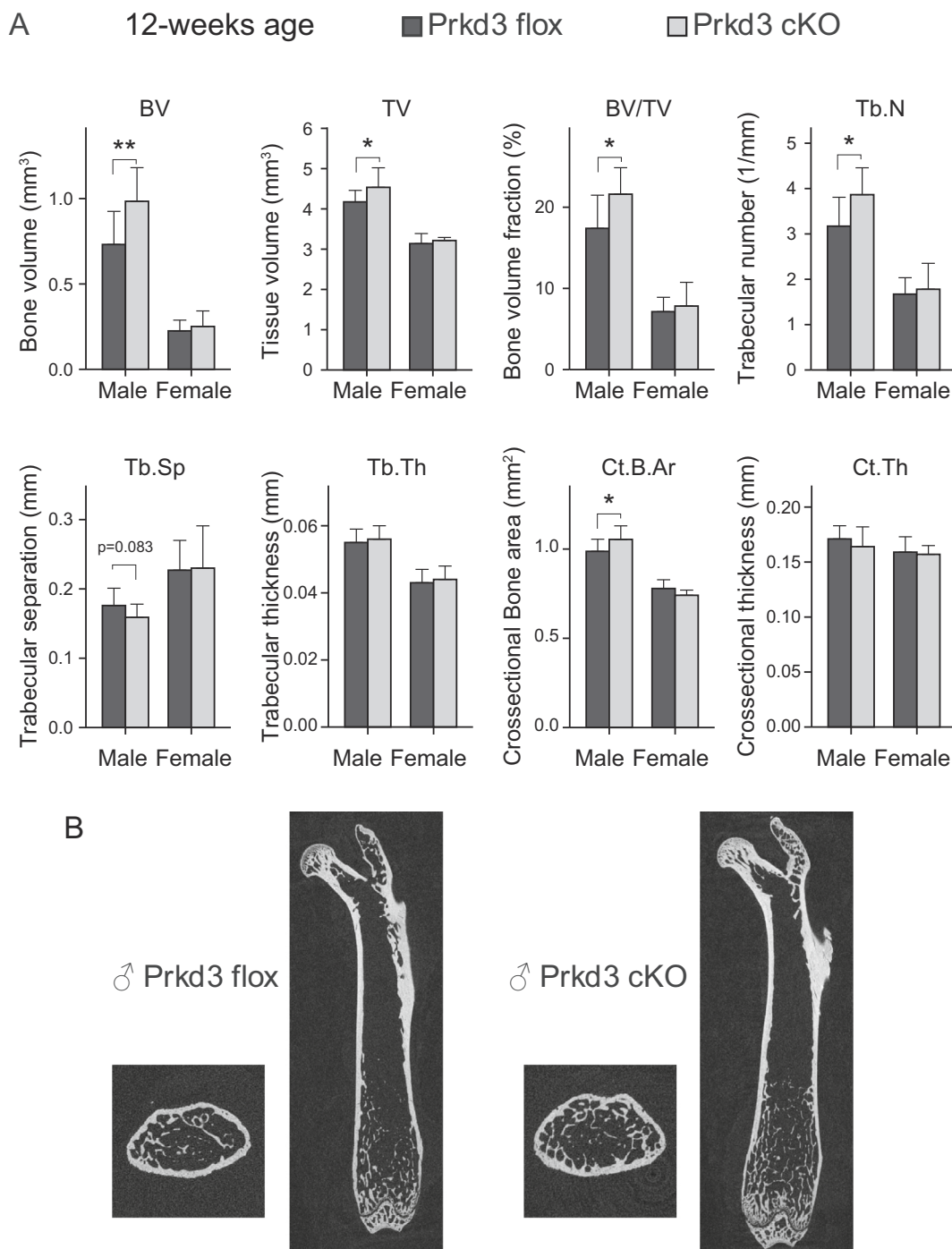


Fig. 4. MicroCT analysis of *Prkd3* cKO femurs at 3 months age (A) μ CT analysis of *Prkd3* flox (dark bars) and *Prkd3* cKO (light bars) mice at 3 months age. Cortical analysis was performed at the mid-diaphysis, while trabecular analysis was done at the distal femur. (B) Sagittal and transverse μ CT images of *Prkd3* femurs. Representative individuals were chosen for having BV/TV near the mean value for their genotype. Number of individuals in each group is given in Fig. 3A. * $p < 0.05$, ** $p < 0.005$.

male cKO mice showed increased trabecular bone measurements, while minimal differences were seen in the cortical bone compartment or in females (Fig. 5). The increased trabecular bone observed in *Prkd3* cKO males is supportive of our working hypothesis, while the lack of phenotype in females was unexpected. We performed histological examination of *Prkd3* bones using H&E and TRAP staining to gain further insights into the cellular mechanisms of their phenotype (Fig. 6A–C). In agreement with the μ CT data, H&E staining at the distal femur in 3-month mice showed a non-statistically significant trend towards 8 % increase in trabecular bone area: tissue area (BA/TA) in male *Prkd3* cKO

(Fig. 6A, C). We examined osteoclasts in these bones by staining for TRAP activity and examining regions within the secondary spongiosa (Fig. 6B). Measurement of the fraction osteoclast perimeter: bone perimeter (Oc.Pm/B.Pm) showed a trend to 31 % reduction in male cKOs ($p = 0.057$) (Fig. 6C). This parameter can be responsive to changes in the number of osteoclasts or in their size. To distinguish between these, we counted the number of osteoclasts per mm of bone perimeter (N.Oc/B.Pm) finding little difference between *Prkd3* flox and cKO (Fig. 6B–C). However, measurement of bone perimeter per individual osteoclast (B.Pm/Oc) showed that the male *Prkd3* cKO cells each

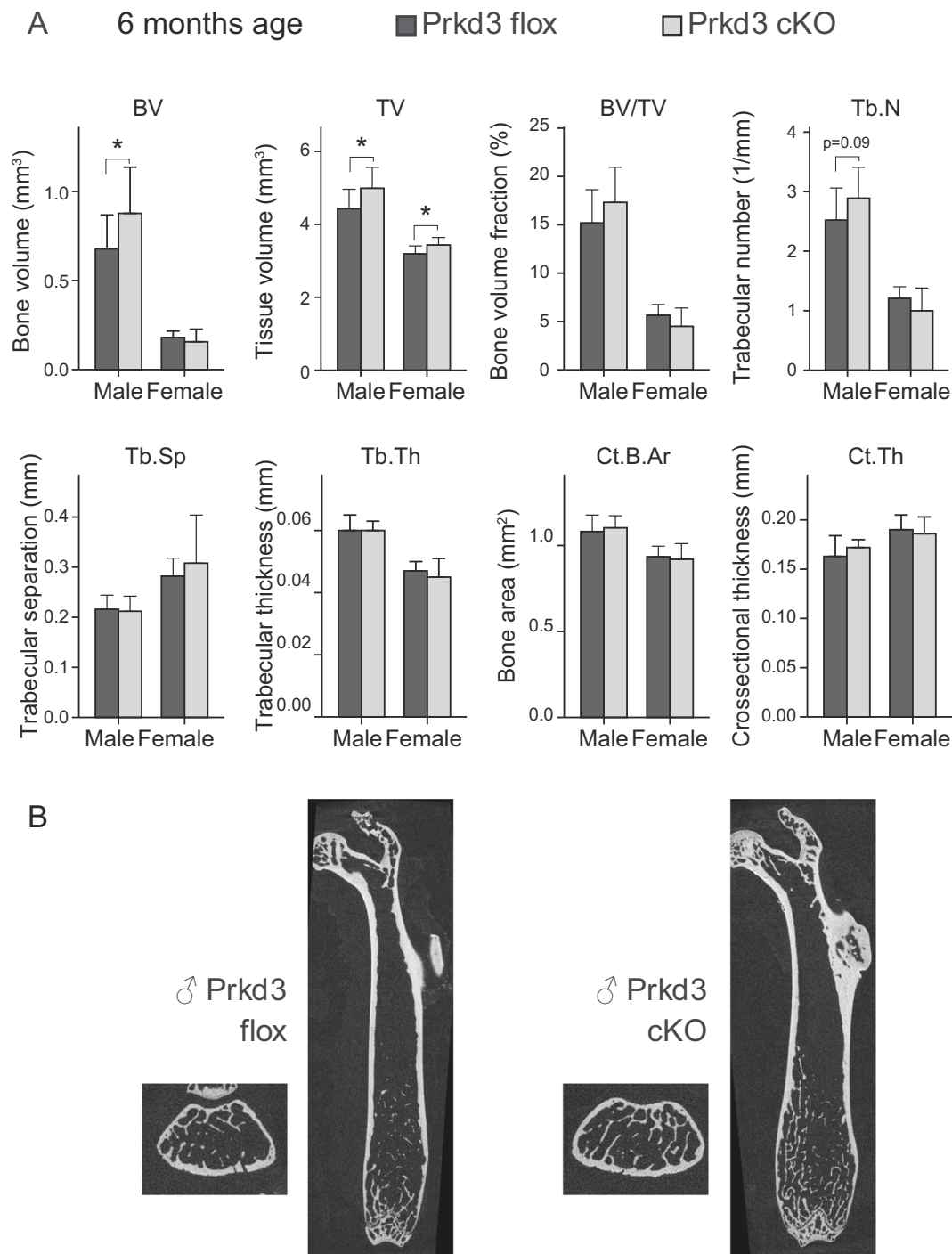


Fig. 5. MicroCT analysis of *Prkd3* cKO femurs at 6 months age (A) μ CT analysis of *Prkd3* flox (dark bars) and *Prkd3* cKO (light bars) mice. Cortical analysis was performed at the mid-diaphysis, while trabecular analysis was done at the distal femur. (B) Sagittal and transverse μ CT images of *Prkd3* femurs. Representative individuals were chosen for having BV/TV near the mean value for their genotype. Number of individuals in each group is given in Fig. 3A. * $p < 0.05$.

covered 55 % less bone perimeter on average than *Prkd3* flox cells ($p = 1.7 \times 10^{-6}$). To quantify the rate of bone resorption in the *Prkd3* mice at 12-weeks, we performed a serum CTX-1 ELISA assay. This assay showed 37.2 ng/mL average CTX-1 for *Prkd3* flox and 30.8 ng/mL for *Prkd3* cKO, a 17 % decrease, which would be consistent with our hypothesis (Fig. 6D). However, this possible difference failed to reach statistical significance so we cannot conclude with confidence that the observed difference was not due to chance. Conversely, female *Prkd3* cKO showed increased CTX-1 compared to flox controls, although this difference was not statistically significant either.

Although our data indicate that PRKD2 is not meaningfully expressed or functionally important in osteoclast cultures, in light of the ambiguities in the *Prkd2* expression data, we proceeded to test for skeletal phenotypes in the *Prkd2* cKO mice. Unlike the skeletal effects of *Prkd3* cKO, we did not detect any phenotype by μ CT analysis of femurs from *Prkd2* conditional knockouts at 1- or 3- month timepoints (Supplemental Fig. 3).

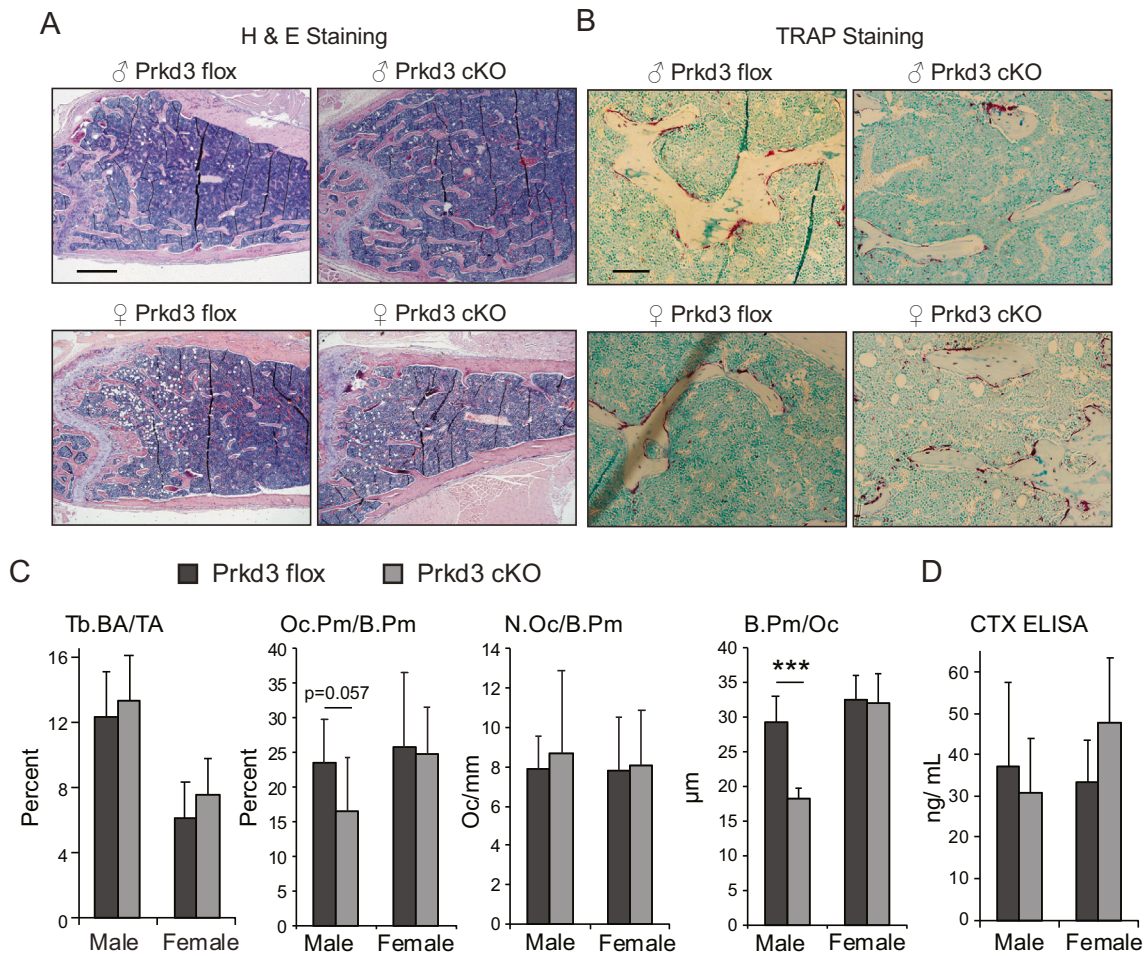


Fig. 6. Histological analysis of *Prkd3* cKO femurs at 3 months age (A) Hematoxylin & eosin (H&E) staining at the distal femur, oriented with the growth plate at the left of the images. Scale bar = 500 μ m (B) TRAP staining (red) with methyl green counterstaining. Scale bar = 100 μ m (C) Morphometric analysis of trabecular bone area/tissue area (Tb.BA/TA), osteoclast perimeter per bone perimeter (Oc.Pm/B.Pm), number of osteoclasts per bone perimeter (N.Oc/B.Pm), and average bone perimeter per individual osteoclast (B.Pm/Oc). (D) CTX-1 ELISA assay performed on serum from *Prkd3* mice at 12 weeks age. *** $p < 0.001$. (For interpretation of the references to colour in this figure legend, the reader is referred to the web version of this article.)

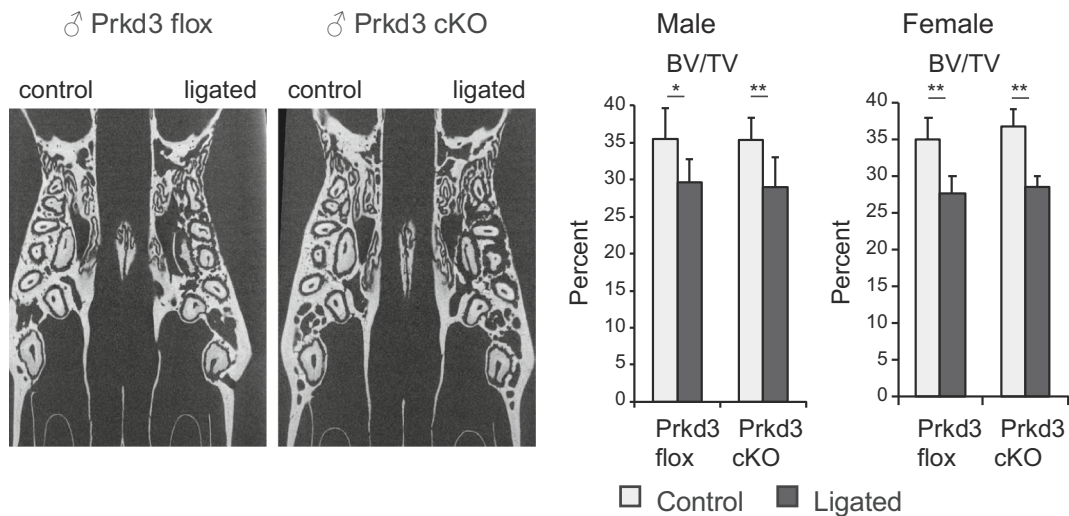


Fig. 7. Periodontal disease model. A ligature was placed around the right second maxillary molar on *Prkd3* mice. After 5 days, the jaws were harvested and imaged using microCT imaging. The amount of bone was measured in a defined region surrounding the roots of the 2nd molars on the ligated and control side of each individual and are graphed as BV/TV. * $p < 0.05$, ** $p < 0.005$.

3.4. Protein kinase D3 cKO does not reduce osteolytic bone loss in a mouse model of periodontitis

To further examine whether PRKD's regulation of osteoclasts might contribute to osteolytic diseases, we utilized a ligature-induced model of periodontitis, with the hypothesis that reduced osteoclast function might reduce bone destruction in *Prkd3* cKO mice. In this model, ligatures are tied around the right second maxillary molar, which is expected to cause inflammation and bone destruction around the ligated tooth. The non-ligated side of each mouse serves as a baseline control. 5 days after ligature placement, we harvested the maxillae and utilized μ CT to measure the extent of bone loss. While bone in the control side of the jaws looked robust and healthy, a loss of bone was readily apparent on the ligated sides (Fig. 7). By comparing the bone volumes in a defined volume-of-interest on the ligated versus non-ligated side of each individual, we determined that *Prkd3* flox males lost 16 % and cKO males lost 18 % of the bone volume in the region of interest. Similar bone destructive effects were seen in females, and again there was no difference observed between flox and cKO. Thus, loss of PRKD3 in osteoclasts does not appear to protect against bone destruction in this model.

4. Discussion

Our previous work revealed that PRKD promotes osteoclasts and bone resorption [20,21]. In those studies, PRKD chemical inhibitors CRT0066101, CID755673 and Gö6976 were shown to have significant inhibitory effects on osteoclast cultures. Since we observed similar effects from multiple different PRKD inhibitors it suggested that the effects were due to PRKD inhibition rather than something off-target. Multiple aspects of osteoclast biology were affected, with defects noted in progression and fusion from mononucleated pre-osteoclasts to multinucleated osteoclasts, in actin ring dynamics, and in the bone resorptive activity of mature osteoclasts. Those studies were limited to *in vitro* cultures, and since they relied on PRKD chemical inhibitors it was not possible to unambiguously distinguish the significance of individual PRKD proteins. To address these limitations and extend our work into the intact living skeleton, in the current study we utilize a novel conditional knockout mouse model system using floxed *Prkd3* and *c-Fms-Cre* to test the hypothesis that loss of PRKD3 in osteoclasts will impair osteoclast formation and function, thereby increasing bone mass.

We are currently focusing primarily on PRKD3 as our data indicate it is the most abundant and important PRKD in osteoclasts. *Prkd3* is readily detected in osteoclasts at the mRNA expression and protein levels. The *cFms-Cre* cKO system gives efficient rearrangement of the *Prkd3* gene, and loss of mRNA and protein. *Prkd3* cKO osteoclast cultures showed abundant but smaller osteoclasts containing fewer nuclei. The osteoclasts that did form exhibited impaired capacity to form or maintain actin rings and a diminished ability to resorb bone *in vitro*. These knockout osteoclast phenotypes were quite similar those seen with PRKD inhibitors [20,21] and further confirm that PRKD, specifically PRKD3, promotes osteoclastogenesis. Our data lean against expression of *Prkd1* or *Prkd2* in osteoclasts. Since there was some ambiguity in the data around PRKD2's expression and we had the mice in hand, we felt it wise to test the effect of knocking it out in osteoclasts. We observed successful genomic DNA deletion and loss of the putative mRNA, but did not see any *in vitro* or *in vivo* skeletal phenotype from *Prkd2* cKO. These results indicate that PRKD2 is not essential and likely not meaningfully expressed in osteoclasts.

Other groups have examined the role of PRKD proteins in myeloid cell types related to osteoclasts, which arise from the monocyte/macrophage branch of the myeloid lineage. All three PRKD genes were detected by RT-PCR in macrophage-like cells including the RAW264.7 cell line and mouse primary macrophages, and effects from *Prkd1* shRNA knockdown in these cells have been described [63–66]. Similarly, knockdown of *Prkd1* showed an effect in neutrophils [67]. PRKD3 was demonstrated to be important in macrophages using a conditional

knockout system driven by *LysM-Cre*, in which the *Prkd3* cKO mice developed lung fibrosis due to altered macrophage activation [68]. Since its expression pattern includes osteoclast progenitor cells, we explored using *LysM-Cre* cKO to verify our results. However, initial studies showed low efficiency in *Prkd3* gene deletion in osteoclast cultures and a weak, inconsistent phenotype, so we did not pursue it further. Similar issues with inadequate knockout in osteoclasts using *LysM-Cre* have been reported by other groups [69,70].

The impaired *Prkd3* cKO *in vitro* osteoclast phenotype leads to our hypothesis that *Prkd3* cKO mice would exhibit reduced osteoclasts and diminished bone resorption, potentially leading to increased bone mass. Indeed, this is what we observed in male *Prkd3* cKO mice, where BV/TV and trabecular number were significantly increased and trabecular separation trended downwards. Histological examination showed similar numbers of osteoclasts per bone perimeter in the trabecular compartment between flox and cKO, but each osteoclast covered less bone surface. Based on the *in vitro* phenotypes, we propose that these *in vivo* differences are likely to be caused by smaller osteoclasts due to impaired precursor fusion, altered cytoskeletal architecture or defective interactions with the bone surface, or perhaps some combination of these. The relationship between total number of osteoclasts and their rate of cell-cell fusion can be complicated since each time two cells fuse together it reduces the number of individual cells, so impaired fusion can actually give an increased number of smaller, less nucleated osteoclasts, which seems to be what we observe in *Prkd3* cKO cultures. They form equal or greater number of multinucleated osteoclasts, but they are smaller with fewer nuclei per cell and show a diminished ability to resorb bone. The *in vivo* skeletal and osteoclast phenotype we observe in *Prkd3* cKO males is somewhat mild, with a normal number of osteoclasts present, but appearing smaller than in control mice, and a modest increase in trabecular bone. These observations suggest to us that PRKD3 functions not as a binary 'on-off' switch absolutely required for osteoclast formation, but more as a dimmer-switch to allow for fine-tuning the level of osteoclast formation and bone resorption in response to varying physiological demands.

Why does *Prkd3* cKO give different skeletal phenotypes between male and female mice, particularly since we don't note a sex difference in culture? Sex-based differences in osteoclasts are established in the literature [71], arising through actions of estrogens and androgens, differences in immune responsiveness and inflammation, further shaped by additional differential gene expression, and likely influenced by signals from osteocytes, osteoblasts or other immune cells. Intrinsic sex differences in osteoclast cell culture systems have been described in some cases but there are conflicting data, and effects are sensitive to differences in culture methodologies and the precise nature of the osteoclast precursors used [71–74]. *In vivo*, sex hormones are major regulators of skeletal physiology, although their effects are complex, implicate multiple cell types, and depend on both the individual's sex and the specific skeletal compartment being considered [75,76]. Loss of estrogens is the major driver of osteoporosis pathogenesis [77]. One component of estrogen's actions involves directly promoting osteoclast apoptosis through estrogen receptor α (ER α) [70,78,79]. Conditional deletion of ER α in osteoclasts increased osteoclastogenesis and bone resorption in female mice, demonstrating that estrogens are protective of trabecular bone *via* direct effects on osteoclasts [70,79]. Despite this inhibitory effect of estrogen, young female C57Bl/6 mice are reported to have increased numbers of osteoclasts in their bones and decreased bone mass relative to males, which is thought to arise due to increased expression of RANKL and enhanced inflammatory signaling pathways stimulating osteoclast formation [72]. Unlike in females, deletion of ER α in mature osteoclasts does not cause trabecular bone loss in male mice [79]. Instead, androgens seem to be the main sex hormones influencing trabecular bone mass in males. Disruption of the androgen receptor (AR) reduces trabecular bone mass, but combined loss of AR and ER α does not give any further bone loss [80]. These effects of androgens on trabecular bone are largely mediated through osteogenic effects on osteocytes and

osteoblasts. Direct effects of androgens in osteoclasts are controversial. Osteoclast-lineage cells do seem to express the AR [81], although its expression level is low compared to osteoblasts and osteocytes. Some papers have reported inhibitory effects of androgens on cultured osteoclasts *in vitro* [82,83]. Other groups report no direct effect of androgens on osteoclasts *in vitro* and no discernable phenotype in either cortical or trabecular bone following conditional knockout of AR in myeloid cells and osteoclasts using *LysM-Cre* or *Ctsk-Cre* [84,85]. *In vitro* osteoclast culture systems are highly simplified models of osteoclastogenesis driven mainly by M-CSF and RANK Ligand, and generally lacking influences from sex hormones, inflammatory cytokines and other regulators present *in vivo*. Under these circumstances, our data indicate that loss of PRKD3 is sufficient to impact osteoclast formation and function. We speculate that in the female skeleton under normal physiological conditions and in the highly inflammatory milieu of the periodontitis model, additional regulatory inputs such as heightened RANKL and inflammatory signals supersede the effects of PRKD3 deletion and promote osteoclast formation and bone resorption.

In summary our current data indicate that PRKD3 is an important factor to enhance osteoclast formation and activity. An exciting possibility originating from the findings that loss of PRKD3 expression or treatment with PRKD inhibitors reduce osteoclasts and bone resorption is that PRKD inhibitors might be clinically useful as antiresorptive agents to reduce bone loss in osteolytic conditions. This possibility needs to be weighed against PRKD's broadly distributed expression, which raises concerns about potential side-effects in other tissues. More specific to the skeleton, there is literature showing PRKD acts in osteoblasts to promote osteogenesis [41,42,86–90], which could imply that any gain in bone health due to anti-osteoclast and anti-resorptive actions of PRKD inhibitors might be offset by decreased bone formation. On the other hand, several groups have made use of PRKD inhibitors in mice against tumor xenografts without noting any adverse effects [91–94], and PRKD inhibitors are being actively investigated as possible anticancer agents [28,46,91,95]. More data are needed to directly test these ideas and explore any possible applications to skeletal physiology and pathology.

Supplementary data to this article can be found online at <https://doi.org/10.1016/j.bone.2023.116759>.

CRediT authorship contribution statement

Samuel D. Burciaga: Investigation, Formal analysis. **Flavia Saavedra:** Investigation. **Lori Fischer:** Investigation. **Karen Johnstone:** Conceptualization, Supervision. **Eric D. Jensen:** Conceptualization, Supervision, Formal analysis, Writing – original draft.

Declaration of competing interest

None.

Data availability

Data underlying this manuscript are available from the corresponding author upon reasonable request.

Acknowledgements

We thank Ashley Gunderson, UMN Oral Pathology Laboratory, for assistance with preparation of histological specimens.

Funding

This work was supported by funds provided through the University of Minnesota School of Dentistry to EDJ.

References

- [1] D.V. Novack, G. Mbalaviele, Osteoclasts-key players in skeletal health and disease, *Microbiol. Spectr.* 4 (3) (2016).
- [2] B.F. Boyce, Advances in the regulation of osteoclasts and osteoclast functions, *J. Dent. Res.* 92 (10) (2013) 860–867.
- [3] T. Ono, T. Nakashima, Recent advances in osteoclast biology, *Histochem. Cell Biol.* 149 (4) (2018) 325–341.
- [4] H. Takayanagi, RANKL as the master regulator of osteoclast differentiation, *J. Bone Miner. Metab.* 39 (1) (2021) 13–18.
- [5] H. Kodama, M. Nose, S. Niida, A. Yamasaki, Essential role of macrophage colony-stimulating factor in the osteoclast differentiation supported by stromal cells, *J. Exp. Med.* 173 (5) (1991) 1291–1294.
- [6] W. Wiktor-Jedrzejczak, A. Bartocci, A.W. Ferrante Jr., A. Ahmed-Ansari, K.W. Sell, J.W. Pollard, E.R. Stanley, Total absence of colony-stimulating factor 1 in the macrophage-deficient osteopetrotic (op/op) mouse, *Proc. Natl. Acad. Sci. U. S. A.* 87 (12) (1990) 4828–4832.
- [7] C.A. O'Brien, T. Nakashima, H. Takayanagi, Osteocyte control of osteoclastogenesis, *Bone* 54 (2) (2013) 258–263.
- [8] L. Danks, N. Komatsu, M.M. Guerrini, S. Sawa, M. Armaka, G. Kollias, T. Nakashima, H. Takayanagi, RANKL expressed on synovial fibroblasts is primarily responsible for bone erosions during joint inflammation, *Ann. Rheum. Dis.* 75 (6) (2016) 1187–1195.
- [9] M. Tsukasaki, H. Takayanagi, Osteoimmunology: evolving concepts in bone-immune interactions in health and disease, *Nat. Rev. Immunol.* 19 (10) (2019) 626–642.
- [10] G. Mori, P. D'Amelio, R. Faccio, G. Brunetti, The interplay between the bone and the immune system, *Clin. Dev. Immunol.* 2013 (2013), 720504.
- [11] T. Koga, M. Inui, K. Inoue, S. Kim, A. Suematsu, E. Kobayashi, T. Iwata, H. Ohnishi, T. Matozaki, T. Kodama, T. Taniguchi, H. Takayanagi, T. Takai, Costimulatory signals mediated by the ITAM motif cooperate with RANKL for bone homeostasis, *Nature* 428 (6984) (2004) 758–763.
- [12] H. Takayanagi, S. Kim, T. Koga, H. Nishina, M. Isshiki, H. Yoshida, A. Saiura, M. Isobe, T. Yokochi, J. Inoue, E.F. Wagner, T.W. Mak, T. Kodama, T. Taniguchi, Induction and activation of the transcription factor NFATc1 (NFAT2) integrate RANKL signaling in terminal differentiation of osteoclasts, *Dev. Cell* 3 (6) (2002) 889–901.
- [13] M. Asagiri, K. Sato, T. Usami, S. Ochi, H. Nishina, H. Yoshida, I. Morita, E. F. Wagner, T.W. Mak, E. Serfling, H. Takayanagi, Autoamplification of NFATc1 expression determines its essential role in bone homeostasis, *J. Exp. Med.* 202 (9) (2005) 1261–1269.
- [14] S. Schmidt, I. Nakhbandi, R. Ruppert, N. Kawelke, M.W. Hess, K. Pfaller, P. Jurdic, R. Fassler, M. Moser, Kindlin-3-mediated signaling from multiple integrin classes is required for osteoclast-mediated bone resorption, *J. Cell Biol.* 192 (5) (2011) 883–897.
- [15] F.P. Ross, S.L. Teitelbaum, alphavbeta3 and macrophage colony-stimulating factor: partners in osteoclast biology, *Immunol. Rev.* 208 (2005) 88–105.
- [16] J. Takito, S. Inoue, M. Nakamura, The sealing zone in osteoclasts: a self-organized structure on the bone, *Int. J. Mol. Sci.* 19 (4) (2018).
- [17] D. Georgess, I. Machuca-Gayet, A. Blangy, P. Jurdic, Podosome organization drives osteoclast-mediated bone resorption, *Cell Adhes. Migr.* 8 (3) (2014) 191–204.
- [18] N.S. Soysa, N. Alles, Osteoclast function and bone-resorbing activity: an overview, *Biochem. Biophys. Res. Commun.* 476 (3) (2016) 115–120.
- [19] A. Bruzzaniti, R. Baron, Molecular regulation of osteoclast activity, *Rev. Endocr. Metab. Disord.* 7 (1–2) (2006) 123–139.
- [20] A.C. Leightner, C.Mello Guimaraes Meyers, M.D. Evans, K.C. Mansky, R. Gopalakrishnan, E.D. Jensen, Regulation of osteoclast differentiation at multiple stages by protein kinase D family kinases, *Int. J. Mol. Sci.* 21 (3) (2020).
- [21] K.C. Mansky, E.D. Jensen, J. Davidova, M. Yamamoto, R. Gopalakrishnan, Protein kinase D promotes *in vitro* osteoclast differentiation and fusion, *J. Biol. Chem.* 288 (14) (2013) 9826–9834.
- [22] C.M.G. Meyers, S.D. Burciaga, B. Faulkner, P. Kazemi, J.M. Cohn, K.C. Mansky, E. D. Jensen, Histone deacetylase 5 is a phosphorylation substrate of protein kinase D in osteoclasts, *Bone* 159 (2022), 116393.
- [23] A.M. Valverde, J. Sinnott-Smith, J. Van Lint, E. Rozengurt, Molecular cloning and characterization of protein kinase D: a target for diacylglycerol and phorbol esters with a distinctive catalytic domain, *Proc. Natl. Acad. Sci. U. S. A.* 91 (18) (1994) 8572–8576.
- [24] F.J. Johannes, J. Prestle, S. Eis, P. Oberhagemann, K. Pfizenmaier, PKC ζ is a novel, atypical member of the protein kinase C family, *J. Biol. Chem.* 269 (8) (1994) 6140–6148.
- [25] S. Sturany, J. Van Lint, F. Muller, M. Wilda, H. Hameister, M. Hocker, A. Brey, U. Gern, J. Vandenheede, T. Gress, G. Adler, T. Seufferlein, Molecular cloning and characterization of the human protein kinase D2. A novel member of the protein kinase D family of serine threonine kinases, *J. Biol. Chem.* 276 (5) (2001) 3310–3318.
- [26] A. Hayashi, N. Seki, A. Hattori, S. Kozuma, T. Saito, PKC ν , a new member of the protein kinase C family, composes a fourth subfamily with PKC μ , *Biochim. Biophys. Acta* 1450 (1) (1999) 99–106.
- [27] G. Manning, D.B. Whyte, R. Martinez, T. Hunter, S. Sudarsanam, The protein kinase complement of the human genome, *Science* 298 (5600) (2002) 1912–1934.
- [28] A. Roy, J. Ye, F. Deng, Q.J. Wang, Protein kinase D signaling in cancer: a friend or foe? *Biochim. Biophys. Acta Rev. Cancer* 1868 (1) (2017) 283–294.
- [29] E. Rozengurt, Protein kinase D signaling: multiple biological functions in health and disease, *Physiology (Bethesda)* 26 (1) (2011) 23–33.

- [30] X. Zhang, J. Connelly, Y. Chao, Q.J. Wang, Multifaceted functions of protein kinase D in pathological processes and human diseases, *Biomolecules* 11 (3) (2021).
- [31] E. Rozengurt, O. Rey, R.T. Waldron, Protein kinase D signaling, *J. Biol. Chem.* 280 (14) (2005) 13205–13208.
- [32] Q.J. Wang, PKD at the crossroads of DAG and PKC signaling, *Trends Pharmacol. Sci.* 27 (6) (2006) 317–323.
- [33] T. Iglesias, R.T. Waldron, E. Rozengurt, Identification of in vivo phosphorylation sites required for protein kinase D activation, *J. Biol. Chem.* 273 (42) (1998) 27662–27667.
- [34] R.T. Waldron, E. Rozengurt, Protein kinase C phosphorylates protein kinase D activation loop Ser744 and Ser748 and releases autoinhibition by the pleckstrin homology domain, *J. Biol. Chem.* 278 (1) (2003) 154–163.
- [35] V.O. Rybin, J. Guo, S.F. Steinberg, Protein kinase D1 autophosphorylation via distinct mechanisms at Ser744/Ser748 and Ser916, *J. Biol. Chem.* 284 (4) (2009) 2332–2343.
- [36] S.A. Matthews, E. Rozengurt, D. Cantrell, Characterization of serine 916 as an in vivo autophosphorylation site for protein kinase D/Protein kinase cmu, *J. Biol. Chem.* 274 (37) (1999) 26543–26549.
- [37] M. Cobbaut, R. Derua, H. Doppler, H.J. Lou, S. Vandoninck, P. Storz, B.E. Turk, T. Seufferlein, E. Waelkens, V. Janssens, J. Van Lint, Differential regulation of PKD isoforms in oxidative stress conditions through phosphorylation of a conserved tyr in the P+1 loop, *Sci. Rep.* 7 (1) (2017) 887.
- [38] P. Storz, H. Doppler, F.J. Johannes, A. Toker, Tyrosine phosphorylation of protein kinase D in the pleckstrin homology domain leads to activation, *J. Biol. Chem.* 278 (20) (2003) 17969–17976.
- [39] C. Jamora, N. Yamanouye, J. Van Lint, J. Laudenslager, J.R. Vandenhede, D. J. Faulkner, V. Malhotra, Gbetagamma-mediated regulation of golgi organization is through the direct activation of protein kinase D, *Cell* 98 (1) (1999) 59–68.
- [40] R. Reinhardt, L. Truebestein, H.A. Schmidt, T.A. Leonard, It takes two to tango: activation of protein kinase D by dimerization, *Bioessays* 42 (4) (2020), e1900222.
- [41] E.D. Jensen, R. Gopalakrishnan, J.J. Westendorf, Bone morphogenic protein 2 activates protein kinase D to regulate histone deacetylase 7 localization and repression of Runx2, *J. Biol. Chem.* 284 (4) (2009) 2225–2234.
- [42] J. Lemonnier, C. Ghayor, J. Guicheux, J. Caverzasio, Protein kinase C-independent activation of protein kinase D is involved in BMP-2-induced activation of stress mitogen-activated protein kinases JNK and p38 and osteoblastic cell differentiation, *J. Biol. Chem.* 279 (1) (2004) 259–264.
- [43] K. Nishikawa, A. Toker, F.J. Johannes, Z. Songyang, L.C. Cantley, Determination of the specific substrate sequence motifs of protein kinase C isozymes, *J. Biol. Chem.* 272 (2) (1997) 952–960.
- [44] H. Döppler, P. Storz, J. Li, M.J. Comb, A. Toker, A phosphorylation state-specific antibody recognizes Hsp27, a novel substrate of protein kinase D, *J. Biol. Chem.* 280 (15) (2005) 15013–15019.
- [45] M.A. Olayioye, S. Barisic, A. Hausser, Multi-level control of actin dynamics by protein kinase D, *Cell. Signal.* 25 (9) (2013) 1739–1747.
- [46] N. Durand, S. Borges, P. Storz, Protein kinase D enzymes as regulators of EMT and cancer cell invasion, *J. Clin. Med.* 5 (2) (2016).
- [47] I. Youssef, J.M. Ricort, Deciphering the role of protein kinase D1 (PKD1) in cellular proliferation, *Mol. Cancer Res.* 17 (10) (2019) 1961–1974.
- [48] Y. Wakana, F. Campelo, The PKD-dependent biogenesis of TGN-to-plasma membrane transport carriers, *Cells* 10 (7) (2021).
- [49] N. Azoitei, M. Cobbaut, A. Becher, J. Van Lint, T. Seufferlein, Protein kinase D2: a versatile player in cancer biology, *Oncogene* 37 (10) (2018) 1263–1278.
- [50] Y. Liu, H. Song, Y. Zhou, X. Ma, J. Xu, Z. Yu, L. Chen, The oncogenic role of protein kinase D3 in cancer, *J. Cancer* 12 (3) (2021) 735–739.
- [51] P. Gilles, L. Voets, J. Van Lint, W.M. De Borggraeve, Developments in the discovery and Design of Protein Kinase D Inhibitors, *ChemMedChem* 16 (14) (2021) 2158–2171.
- [52] E. Ishikawa, H. Kosako, T. Yasuda, M. Ohmura, K. Araki, T. Kurosaki, T. Saito, S. Yamasaki, Protein kinase D regulates positive selection of CD4(+) thymocytes through phosphorylation of SHP-1, *Nat. Commun.* 7 (2016) 12756.
- [53] L. Xing, B.F. Boyce, RANKL-based osteoclastogenic assays from murine bone marrow cells, *Methods Mol. Biol.* 1130 (2014) 307–313.
- [54] S. Takeshita, K. Kaji, A. Kudo, Identification and characterization of the new osteoclast progenitor with macrophage phenotypes being able to differentiate into mature osteoclasts, *J. Bone Miner. Res.* 15 (8) (2000) 1477–1488.
- [55] I.R. Orriss, T.R. Arnett, Rodent osteoclast cultures, *Methods Mol. Biol.* 816 (2012) 103–117.
- [56] T. Tamura, N. Takahashi, T. Akatsu, T. Sasaki, N. Udagawa, S. Tanaka, T. Suda, New resorption assay with mouse osteoclast-like multinucleated cells formed in vitro, *J. Bone Miner. Res.* 8 (8) (1993) 953–960.
- [57] K.F. Johnstone, Y. Wei, P.D. Bittner-Eddy, G.W. Vreeman, I.A. Stone, J.B. Clayton, C.S. Reilly, T.B. Walbon, E.N. Wright, S.L. Hoops, W.S. Boyle, M. Costalonga, M. C. Herzberg, Calprotectin (S100A8/A9) is an innate immune effector in experimental periodontitis, *Infect. Immun.* 89 (10) (2021), e0012221.
- [58] L. Deng, J.F. Zhou, R.S. Sellers, J.F. Li, A.V. Nguyen, Y. Wang, A. Orlofsky, Q. Liu, D.A. Hume, J.W. Pollard, L. Augenlicht, E.Y. Lin, A novel mouse model of inflammatory bowel disease links mammalian target of rapamycin-dependent hyperproliferation of colonic epithelium to inflammation-associated tumorigenesis, *Am. J. Pathol.* 176 (2) (2010) 952–967.
- [59] V. Choudhary, L.O. Olala, I. Kaddour-Djebbar, I. Helwa, W.B. Bollag, Protein kinase D1 deficiency promotes differentiation in epidermal keratinocytes, *J. Dermatol. Sci.* 76 (3) (2014) 186–195.
- [60] M. Ernest Dodd, V.L. Ristich, S. Ray, R.M. Lober, W.B. Bollag, Regulation of protein kinase D during differentiation and proliferation of primary mouse keratinocytes, *J. Investig. Dermatol.* 125 (2) (2005) 294–306.
- [61] V.L. Ristich, P.H. Bowman, M.E. Dodd, W.B. Bollag, Protein kinase D distribution in normal human epidermis, basal cell carcinoma and psoriasis, *Br. J. Dermatol.* 154 (4) (2006) 586–593.
- [62] V. Ryvkin, M. Raschel, T. Gaddapara, S. Ghazizadeh, Opposing growth regulatory roles of protein kinase D isoforms in human keratinocytes, *J. Biol. Chem.* 290 (17) (2015) 11199–11208.
- [63] Y.I. Kim, J.E. Park, D.D. Brand, E.A. Fitzpatrick, A.K. Yi, Protein kinase D1 is essential for the proinflammatory response induced by hypersensitivity pneumonitis-causing thermophilic actinomyces *saccharopolyspora rectivirgula*, *J. Immunol.* 184 (6) (2010) 3145–3156.
- [64] J.E. Park, Y.I. Kim, A.K. Yi, Protein kinase D1: a new component in TLR9 signaling, *J. Immunol.* 181 (3) (2008) 2044–2055.
- [65] J.E. Park, Y.I. Kim, A.K. Yi, Protein kinase D1 is essential for MyD88-dependent TLR signaling pathway, *J. Immunol.* 182 (10) (2009) 6316–6327.
- [66] K. Upadhyay, J.E. Park, T.W. Yoon, P. Halder, Y.I. Kim, V. Metcalfe, A.J. Talati, B. K. English, A.K. Yi, Group B streptococci induce proinflammatory responses via a protein kinase D1-dependent pathway, *J. Immunol.* 198 (11) (2017) 4448–4457.
- [67] A. Ittner, H. Block, C.A. Reichel, M. Varjosalo, H. Gehart, G. Sumara, M. Gstaiger, F. Krombach, A. Zarbock, R. Ricci, Regulation of PTEN activity by p38delta-PKD1 signaling in neutrophils confers inflammatory responses in the lung, *J. Exp. Med.* 209 (12) (2012) 2229–2246.
- [68] S. Zhang, H. Liu, M. Yin, X. Pei, A. Hausser, E. Ishikawa, S. Yamasaki, Z.G. Jin, Deletion of protein kinase D3 promotes liver fibrosis in mice, *Hepatology* 72 (5) (2020) 1717–1734.
- [69] A.O. Aliprantis, Y. Ueki, R. Sulyanto, A. Park, K.S. Sigrist, S.M. Sharma, M. C. Ostrowski, B.R. Olsen, L.H. Glimcher, NFATc1 in mice represses osteoprotegerin during osteoclastogenesis and dissociates systemic osteopenia from inflammation in cherubism, *J. Clin. Invest.* 118 (11) (2008) 3775–3789.
- [70] M. Martin-Millan, M. Almeida, E. Ambrogini, L. Han, H. Zhao, R.S. Weinstein, R. L. Jilka, C.A. O'Brien, S.C. Manolagas, The estrogen receptor-alpha in osteoclasts mediates the protective effects of estrogens on cancellous but not cortical bone, *Mol. Endocrinol.* 24 (2) (2010) 323–334.
- [71] J. Lorenzo, Sexual dimorphism in osteoclasts, *Cells* 9 (9) (2020).
- [72] S.H. Mun, S. Jastrzebski, J. Kalinowski, S. Zeng, B. Oh, S. Bae, G. Eugenia, N. M. Khan, H. Drissi, P. Zhou, B. Shin, S.K. Lee, J. Lorenzo, K.H. Park-Min, Sexual dimorphism in differentiating osteoclast precursors demonstrates enhanced inflammatory pathway activation in female cells, *J. Bone Miner. Res.* 36 (6) (2021) 1104–1116.
- [73] M.S. Valerio, D.S. Basilakos, J.E. Kirkpatrick, M. Chavez, J. Hathaway-Schrader, B. A. Herbert, K.L. Kirkwood, Sex-based differential regulation of bacterial-induced bone resorption, *J. Periodontol. Res.* 52 (3) (2017) 377–387.
- [74] A. Zarei, C. Yang, J. Gibbs, J.L. Davis, A. Ballard, R. Zeng, L. Cox, D.J. Veis, Manipulation of the alternative NF-kappaB pathway in mice has sexually dimorphic effects on bone, *JBMR Plus* 3 (1) (2019) 14–22.
- [75] F. Callewaert, M. Sinnesael, E. Gielen, S. Boonen, D. Vanderschueren, Skeletal sexual dimorphism: relative contribution of sex steroids, GH-IGF1, and mechanical loading, *J. Endocrinol.* 207 (2) (2010) 127–134.
- [76] M. Laurent, L. Antonio, M. Sinnesael, V. Dubois, E. Gielen, F. Claessens, D. Vanderschueren, Androgens and estrogens in skeletal sexual dimorphism, *Asian J. Androl.* 16 (2) (2014) 213–222.
- [77] S. Khosla, M.J. Oursler, D.G. Monroe, Estrogen and the skeleton, *Trends Endocrinol. Metab.* 23 (11) (2012) 576–581.
- [78] T. Kameda, H. Mano, T. Yuasa, Y. Mori, K. Miyazawa, M. Shiokawa, Y. Nakamura, E. Hiroi, K. Hiura, A. Kameda, N.N. Yang, Y. Hakeda, M. Kumegawa, Estrogen inhibits bone resorption by directly inducing apoptosis of the bone-resorbing osteoclasts, *J. Exp. Med.* 186 (4) (1997) 489–495.
- [79] T. Nakamura, Y. Imai, T. Matsumoto, S. Sato, K. Takeuchi, K. Igarashi, Y. Harada, Y. Azuma, A. Krust, Y. Yamamoto, H. Nishina, S. Takeda, H. Takayanagi, D. Metzger, J. Kanno, K. Takaoka, T.J. Martin, P. Chambon, S. Kato, Estrogen prevents bone loss via estrogen receptor alpha and induction of fas ligand in osteoclasts, *Cell* 130 (5) (2007) 811–823.
- [80] F. Callewaert, K. Venken, J. Ophoff, K. De Gendt, A. Torcasio, G.H. van Lenthe, H. Van Oosterwyck, S. Boonen, R. Bouillon, F. Verhoeven, D. Vanderschueren, Differential regulation of bone and body composition in male mice with combined inactivation of androgen and estrogen receptor-alpha, *FASEB J.* 23 (1) (2009) 232–240.
- [81] Y. Mizuno, T. Hosoi, S. Inoue, A. Ikegami, M. Kaneki, Y. Akedo, T. Nakamura, Y. Ouchi, C. Chang, H. Orimo, Immunocytochemical identification of androgen receptor in mouse osteoclast-like multinucleated cells, *Calcif. Tissue Int.* 54 (4) (1994) 325–326.
- [82] H. Michael, P.L. Harkonen, H.K. Vaananen, T.A. Hentunen, Estrogen and testosterone use different cellular pathways to inhibit osteoclastogenesis and bone resorption, *J. Bone Miner. Res.* 20 (12) (2005) 2224–2232.
- [83] L. Pederson, M. Kremer, J. Judd, D. Pascoe, T.C. Spelsberg, B.L. Riggs, M.J. Oursler, Androgens regulate bone resorption activity of isolated osteoclasts in vitro, *Proc. Natl. Acad. Sci. U. S. A.* 96 (2) (1999) 505–510.
- [84] M. Sinnesael, F. Jardi, L. Deboel, M.R. Laurent, V. Dubois, J.D. Zajac, R.A. Davey, G. Carmeliet, F. Claessens, D. Vanderschueren, The androgen receptor has no direct antiresorptive actions in mouse osteoclasts, *Mol. Cell. Endocrinol.* 411 (2015) 198–206.
- [85] S. Ucer, S. Iyer, S.M. Bartell, M. Martin-Millan, L. Han, H.N. Kim, R.S. Weinstein, R. L. Jilka, C.A. O'Brien, M. Almeida, S.C. Manolagas, The effects of androgens on murine cortical bone do not require AR or ERalpha signaling in osteoblasts and osteoclasts, *J. Bone Miner. Res.* 30 (7) (2015) 1138–1149.
- [86] W.B. Bollag, V. Choudhary, Q. Zhong, K.H. Ding, J. Xu, R. Elsayed, K. Yu, Y. Su, L. J. Bailey, X.M. Shi, M. Elsalanty, M.H. Johnson, M.E. McGee-Lawrence, C.M. Isaacs,

- Deletion of protein kinase D1 in osteoprogenitor cells results in decreased osteogenesis in vitro and reduced bone mineral density in vivo, *Mol. Cell. Endocrinol.* 461 (2018) 22–31.
- [87] A.B. Celil, P.G. Campbell, BMP-2 and insulin-like growth factor-1 mediate osterix (Osx) expression in human mesenchymal stem cells via the MAPK and protein kinase D signaling pathways, *J. Biol. Chem.* 280 (36) (2005) 31353–31359.
- [88] W.H. Ha, H.S. Seong, N.R. Choi, B.S. Park, Y.D. Kim, Recombinant human bone morphogenic protein-2 induces the differentiation and mineralization of osteoblastic cells under hypoxic conditions via activation of protein kinase D and p38 mitogen-activated protein kinase signaling pathways, *Tissue Eng. Regen. Med.* 14 (4) (2017) 433–441.
- [89] J.H. Heo, J.H. Choi, I.R. Kim, B.S. Park, Y.D. Kim, Combined treatment with low-level laser and rhBMP-2 promotes differentiation and mineralization of osteoblastic cells under hypoxic stress, *Tissue Eng. Regen. Med.* 15 (6) (2018) 793–801.
- [90] L.C. Yeh, X. Ma, R.W. Matheny, M.L. Adamo, J.C. Lee, Protein kinase D mediates the synergistic effects of BMP-7 and IGF-I on osteoblastic cell differentiation, *Growth Factors* 28 (5) (2010) 318–328.
- [91] S. Borges, E.A. Perez, E.A. Thompson, D.C. Radisky, X.J. Geiger, P. Storz, Effective targeting of estrogen receptor-negative breast cancers with the protein kinase D inhibitor CRT0066101, *Mol. Cancer Ther.* 14 (6) (2015) 1306–1316.
- [92] K.B. Harikumar, A.B. Kunnumakkara, N. Ochi, Z. Tong, A. Deorukhkar, B. Sung, L. Kelland, S. Jamieson, R. Sutherland, T. Raynham, M. Charles, A. Bagherzadeh, C. Foxton, A. Boakes, M. Farooq, D. Maru, P. Diagaradjane, Y. Matsuo, J. Sinnott-Smith, J. Gelovani, S. Krishnan, B.B. Aggarwal, E. Rozengurt, C.R. Ireson, S. Guha, A novel small-molecule inhibitor of protein kinase D blocks pancreatic cancer growth in vitro and in vivo, *Mol. Cancer Ther.* 9 (5) (2010) 1136–1146.
- [93] Y. Liu, Y. Wang, S. Yu, Y. Zhou, X. Ma, Q. Su, L. An, F. Wang, A. Shi, J. Zhang, L. Chen, The role and mechanism of CRT0066101 as an effective drug for treatment of triple-negative breast cancer, *Cell. Physiol. Biochem.* 52 (3) (2019) 382–396.
- [94] N. Wei, E. Chu, P. Wipf, J.C. Schmitz, Protein kinase d as a potential chemotherapeutic target for colorectal cancer, *Mol. Cancer Ther.* 13 (5) (2014) 1130–1141.
- [95] C.R. LaValle, K.M. George, E.R. Sharlow, J.S. Lazo, P. Wipf, Q.J. Wang, Protein kinase D as a potential new target for cancer therapy, *Biochim. Biophys. Acta* 1806 (2) (2010) 183–192.